Supplementary Information for

Distinct regimes of particle and virus abundance explain face mask efficacy for COVID-19.

Yafang Cheng[1,2], Nan Ma[2], Christian Witt, Steffen Rapp, Philipp Wild, Meinrat O. Andreae, Ulrich Pöschl, Hang Su[1].

[1] Correspondence to: H.S. (h.su@mpic.de) and Y.C. (yafang.cheng@mpic.de)

Email: h.su@mpic.de and yafang.cheng@mpic.de

[2] These authors contributed equally to this work.

This PDF file includes:

Supplementary text S1 to S3
Figures S1 to S10
Tables S1 to S7
SI References

Supplementary Text

S1. Scenarios in Leung et al. (2020)

Leung et al. (2020) reported an average of 5 to 17 coughs during 30-min exhaled breath collection for virus-infected participants (1). Taking the particle size distribution given in Fig. 2, we calculate that one person can emit a total number of 9.31×10^5 to 2.72×10^6 particles in a 30 min sampling period. Note that particles > 100 μm were not considered here, and the volume concentrations of particles in the "droplet" mode (2.44×10^{-4} mL, with 4.29×10^{-5} to 2.45×10^{-3} mL in 5% to 95% confidence level) overwhelm those in the "aerosol" mode (7.68×10^{-7} mL, with 3.37×10^{-7} to 5.24×10^{-6} mL in 5% to 95% confidence level).

S2. Virus concentration

S2.1 Virus concentration in exhalation samples of Leung et al. (2020)

Many samples in Leung et al. (2020) return a virus number below the detection limit (Fig. S4) (1). To reconstruct the whole distribution, we adopted an alternative approach, using the statistical distribution, i.e., percentage of positive cases, to calculate the virus number. Assuming that the virus number in the samples follows a Poisson distribution, the percentage of positive samples (containing > 2 viruses, i.e., Leung et al., 2020 used $10^{0.3}$# as undetectable values in their statistical analysis) can be calculated with pre-assumed viral load in exhaled liquids. The Poisson distribution of virus number in emitted droplets is supported by early experiments, where the amount of bioaerosols or compounds delivered in particles is proportional to its concentration in the bulk fluid used to generate particles, and it is independent of investigated particulate type (fluorescent bead, bacteria or spore) (2).

For a set of sufficient samples, the positive rate (percentage of samples with virus number N >2) is a function of the mathematical expectation of virus number per sample (N_{me}). The N_{me} therefore can be retrieved by scanning a series of N_{me} until the calculated positive rate agrees with the measurement. It should be noted that the viral load in exhaled liquids and the total exhaled liquid volume may be different among individuals, which must be considered in the calculation. Therefore, the Monte Carlo approach is used in this study. We assume that the statistical number distribution of SARS-CoV-2 in nasopharyngeal and nasal swab samples (Fig. S5, Jacot et al., 2020 (3)) can represent the individual difference of viral load in exhaled liquids. The distributions can be fitted with multi-mode lognormal distribution with a low-abundance mode and a high-abundance mode. The dispersion of the high abundance mode ($\sigma \sim 1$) is adopted in our calculation. In the experiment of Leung et al. (2020), the difference of sampled liquid volume stems from the individual difference of coughing times and volume concentration of exhaled droplets. The coughing time is assumed to follow a normal distribution with a σ of 44.5. The exhaled droplet volume concentration is assumed to follow a lognormal distribution with a σ of $\log_{10}(2)$. The experiment in Leung et al. (2020) is simulated with a series of viral loads. At each viral load, the experiment with the same sample number as in Leung et al. (2020) is repeated for 1×10^5 times to obtain a stable result. For each sample, the mathematical expectation of virus number is calculated based on randomly generated coughing time, exhaled aerosol/droplet volume concentration, and viral load. The "true virus number" in each sample is assumed to follow a Poisson distribution, and is randomly generated with its mathematical expectation equaling to the calculated value. Finally, for each pre-defined viral load, a distribution of positive rates can be obtained and fitted with a normal distribution function. When the calculated median positive rates become equal to the reported values in Leung et al. (2020), the viral load of coronavirus, influenza virus and rhinovirus in exhaled liquids are determined (Table S2), which is then used to calculate the distribution function and median of virus number per sample (Fig. S6 and Table S3).

Given the volume of exhaled liquids in each sample (V_p), the viral load in respiratory tract fluid, $C_{v,fluid}$ (number of viruses per volume of respiratory tract fluid) can be calculated by :

$$C_{V,fluid} = \frac{N_{sample}}{V_p} \quad (1)$$

S2.2 Viral load in respiratory tract fluid of Jacot et al. (2020)

Jacot et al. (2020) presented a large 9-week dataset of viral load in nasopharyngeal and nasal swab samples (3). As shown in Fig. S5, the viral load apparently exhibited a multi-mode lognormal distribution (overall $\sigma \sim 2$), with one low-abundance mode around ~1×10^3 to 1×10^5 copies/mL, and the other high-abundance mode ~1×10^5 to 1×10^{10} copies/mL. The high-abundance mode shows a negative skew lognormal distribution, probably due to the reduced viral load over time. To calculate the infection risks in Fig. 3B, we took the variability of the high abundance mode with $\sigma \sim 1$. The low-abundance mode is not considered due to its much smaller contribution to the infection risk compared to the high-abundance mode.

S3. Effect of wearing masks

We evaluate the effect of wearing masks in controlling the SARS-CoV-2 virus transmission. As detailed below, wearing surgical masks may remove 82% of the SARS-CoV-2 virus. Here, for simplicity, we assume that the percentage change of the virus transmission rate (i.e., the reproductive number) due to airborne transmissions is proportional to the percentage change of transmitted virus numbers. Given a typical reproductive number, R_0, of ~2.5 for COVID-19, wearing a surgical mask can reduce it to ~ 0.46 and thus allow containing the virus. For N95 masks, the reproductive number may even drop to 0.049. This degree of effect is apparently consistent with the real conditions (Fig. S7).

S3.1. Effect of wearing masks on reducing the reproduction number *R* of COVID-19

Wearing surgical or N95 masks can reduce the emission rate of virus and further reduce the reproduction number *R* of COVID-19. Assuming that infectious individuals cough on average 20 times and speak for 10 minutes per hour, the volume emission rate of exhaled droplets ($E_{\text{V-drop}}$) can be calculated based on the size distributions shown in Fig. 2, and the emission rate of virus ($E_{\text{N-virus}}$) can be calculated with the viral load in Table S2. Table S4 shows the results for droplet size range of $D_w < 5$ μm and $D_w < 20$ μm. It can be seen that wearing surgical masks and N95 masks can reduce the emission of virus by 81.7% and 98.0% ($D_w < 20$ μm), respectively.

Assuming that the reproduction number *R* is proportional to the emission rate of virus-containing droplets (4), the effect of wearing masks on *R* can be calculated. Assuming a basic reproduction number R_0 of 2.5, all infectious individuals wearing surgical mask and N95 mask can reduce *R* to 0.46 and 0.049, respectively. It should be noted that only the mask removal of virus from the emitters is considered in the calculation. If all people wear masks, the number of viruses inhaled by healthy people will be further reduced, thereby further reducing *R*.

S3.2. The effect of wearing masks on the outbreak and popularity of COVID-19

To evaluate the effect of wearing masks on the dynamics of the COVID-19 outbreak, the infectious disease dynamics model (SEIR model) is employed to model the number of infections (5):

$$\begin{cases} \frac{dS_p}{dt} = -\frac{\beta_t S_p I_p}{N_p} \\ \frac{dE_p}{dt} = \frac{\beta_t S_p I_p}{N_p} - \sigma_i E_p \\ \frac{dI_p}{dt} = \sigma_i E_p - \gamma_r I_p \\ \frac{dR_p}{dt} = \gamma_r I_p \\ \beta_t = R_0 \gamma_r \end{cases} \quad (2)$$

where N_p is total population, S_p is the susceptible population, E_p is the exposed population, I_p is infectious population, R_p is recovered or dead population, β_t is the transmission rate, σ_i is the infection rate, γ_r is the recovery rate, and R_0 is the basic reproduction number. Zhang et al. (2020) investigated the effect of limiting social contact patterns on the reproduction number of COVID-19 in Wuhan, China (6). We also select Wuhan as the target city, to compare the effects of wearing a mask and limiting social contact patterns reported in Zhang et al. (2020). The parameters in the SEIR model are assumed as follows (6, 7):

- N_p = 11080000;
- γ_r = 0.0556;
- σ_i = 0.1923;
- R_0 = 2.5;
- The first outbreak occurred on December 2, 2019: E_p=3000 and I_p=10.

Assuming that control measures starts on January 24 and no control measures are implemented before January 23, the effects of the following control measures are evaluated with the SEIR model:

- Only school closure: R=1.9 (6);
- Reduce personnel contact (through home isolation, close public settings, etc.): R=0.34 (6);
- Wearing surgical masks, no other measures: R=0.46;
- Wearing N95 masks, no other measures: R=0.049.

Figure S7(A) shows the results of the model calculation. Table S5 shows the cumulative total number of infections and the percentage of total infections under the five scenarios. It can be seen that wearing a surgical/N95 mask can reduce the total infection rate to below 1%, which is similar as limiting social contact patterns. As a sensitivity study, we also calculated the total infection number and infection rate based on different virus emission reduction rates of masks. Results are shown in Fig. S7(B) and Table S6.

S4. Infection probability and infectious dose

To estimate the infection probability of viruses, we need to understand the infection mechanism and relevant parameters. A key question is the minimum number of viruses that can lead to an infection.

In the main text, we assumed one virus as the minimum number and all viruses have the same infection probability. Then the infection probability by a single virus (P_{single}) can be determined from the median infectious dose (ID50), which is the virus number to produce infection in 50% of susceptible people, by $P_{single} = 1 - 10^{\frac{log10(0.5)}{ID50}}$.

In Fig. S8, we have also calculated the case assuming different minimum numbers of viruses (with and without considering the individual differences given in Fig. 3). Though different minimum virus numbers may lead to different P_{inf}-N_{30} relation (Fig. S8A), the large variability caused by individual differences diminishes this effect (Fig. S8B) resulting in a similar relation as in Fig. 3B.

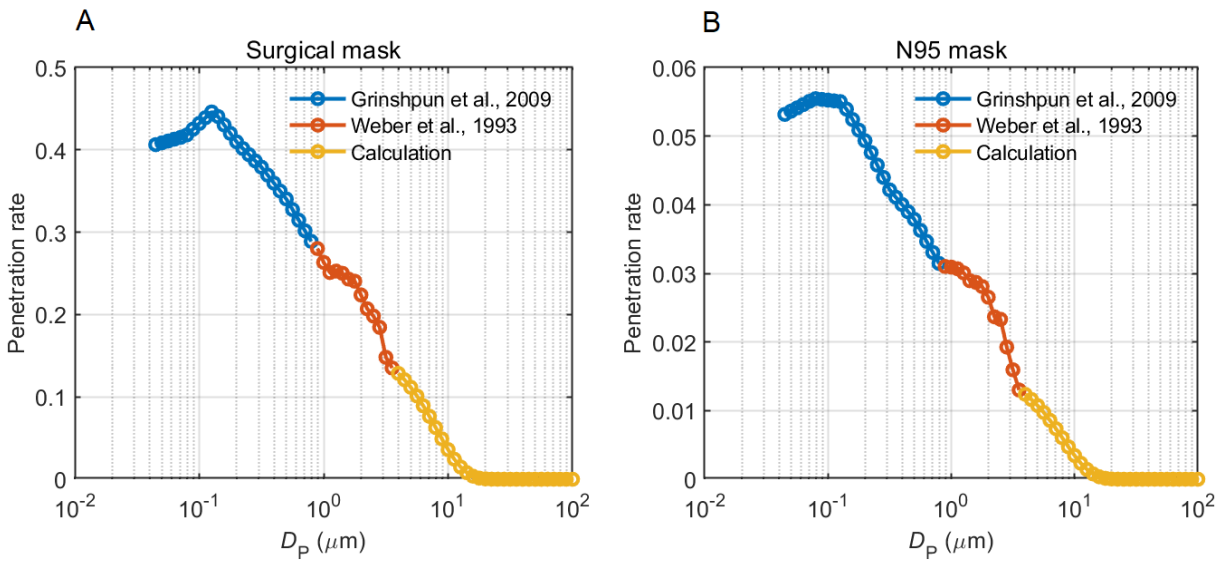

Fig. S1. Particle penetration rate of a surgical mask (A) and a N95 mask (B). For the particle size range of ~50 nm to ~ 800 nm, the penetration rate (blue circle line) is modified from Grinshpun et al. (2009) (8). For particle size range of ~800 nm to ~ 3.5 μm, the penetration rate (red circle line) is modified from Weber et al. (1993) (9). For particle size above ~3.5 μm, the penetration rate (yellow circle line) is calculated based on particle impaction.

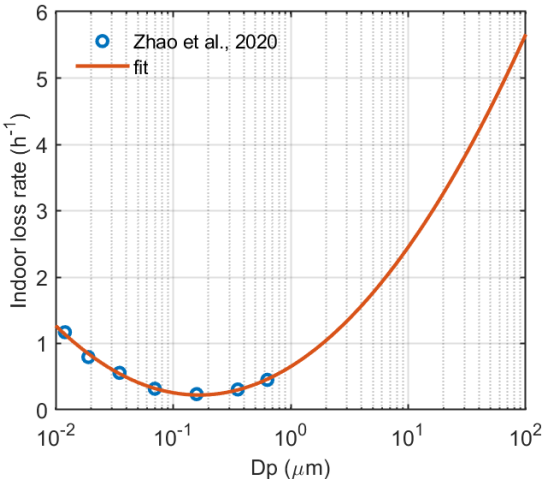

Fig. S2. Size-resolved particle loss rate in indoor environment with natural ventilation. The blue circles represent the measurement in Zhao et al. (2020) (10). The red line shows the fit result with $\lambda = 0.703 \cdot D_P^2 + 1.10 \cdot D_P + 0.651$.

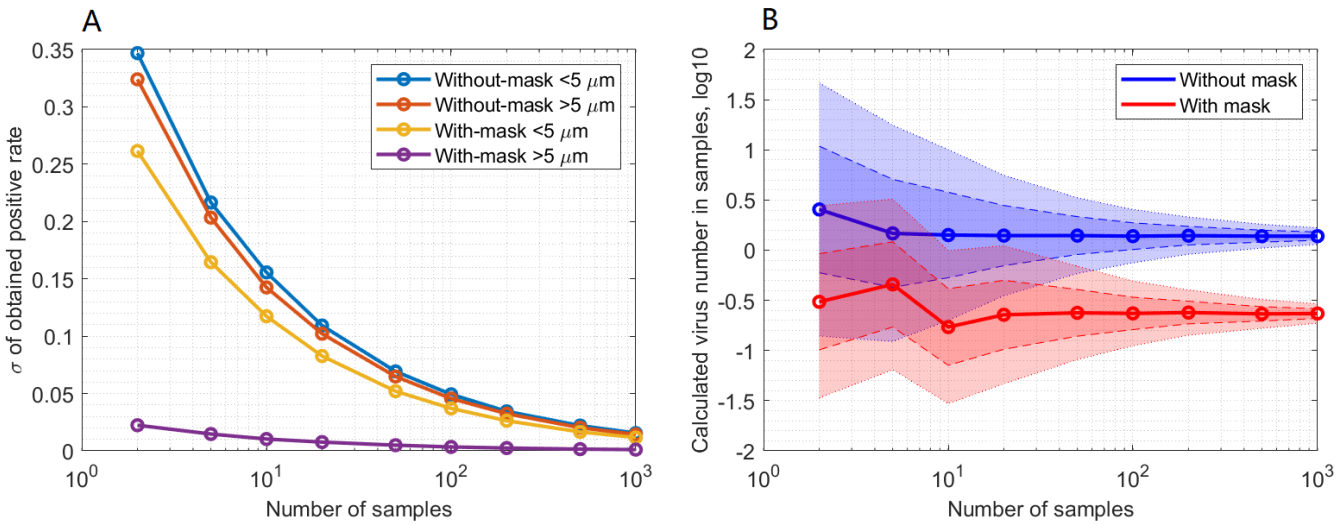

Fig. S3. (**A**) Standard deviation of positive rates derived based on different sample numbers. Four scenarios are tested: aerosol mode (D_w < 5 μm) samples of 30-min exhalation by patients without wearing surgical masks (blue circle line), droplet mode (D_w > 5 μm) samples of 30-min exhalation by patients without wearing surgical masks (red circle line), aerosol mode samples of 30-min exhalation by patients wearing surgical masks (yellow circle line), and droplet mode samples of 30-min exhalation by patients wearing surgical masks (purple circle line). The viral loads in aerosol and droplet mode particles are assumed to be the same as the coronavirus (Table S2). (**B**) Frequency distributions of derived viral load in 30-min exhalation samples at different sample numbers. The solid circle lines show the median viral load. Median ±σ and median±2σ are shown as dashed and dotted lines, respectively. The calculated viral load of coronavirus in aerosol mode (1.39# and 0.682#, Table S3) is adopted as the true viral load in the test. The positive rates of samples are assumed to follow normal distributions with σ shown in panel A.

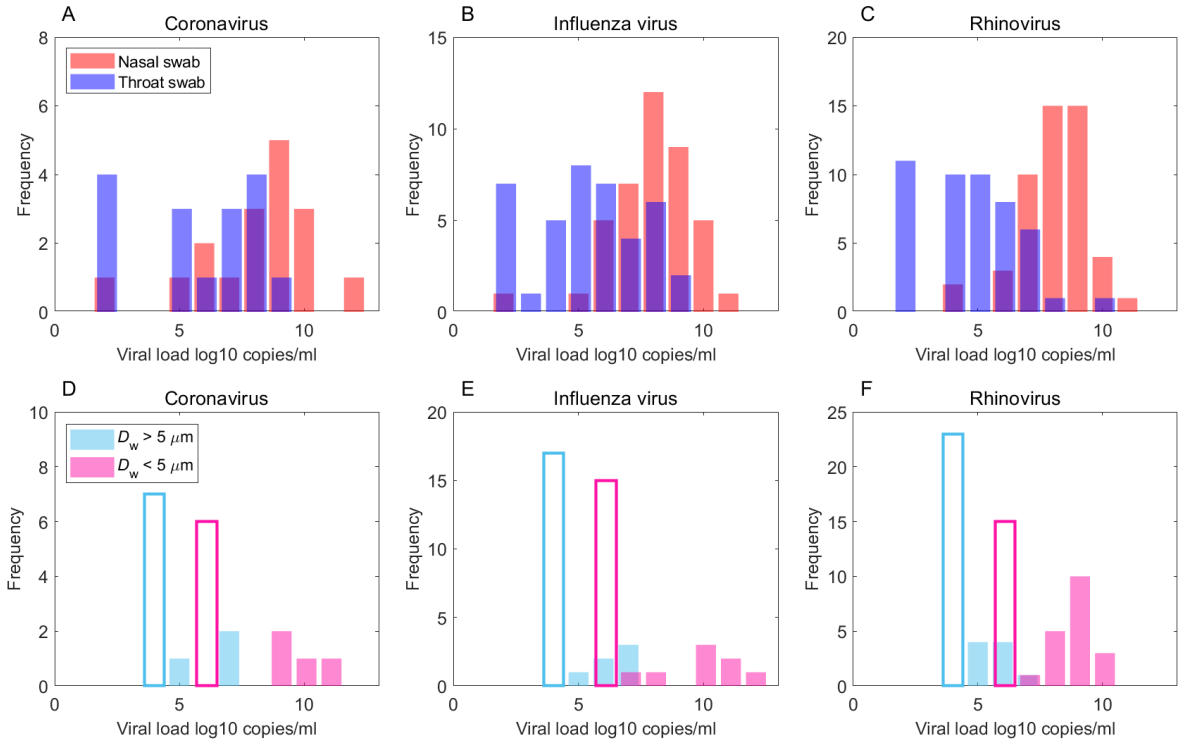

Fig. S4. Frequency distributions of observed virus load in respiratory tract fluid. (**A**), (**B**) and (**C**) show the measured viral load in nasal and throat swabs for coronavirus, influenza virus and rhinovirus, respectively; (**D**), (**E**) and (**F**) show the viral load calculated from virus number of exhalation samples (Eq. 1 in Sect S2). The unshaded bars represent samples with virus number below the detection limit (2 viruses, Leung et al. 2020 (1)).

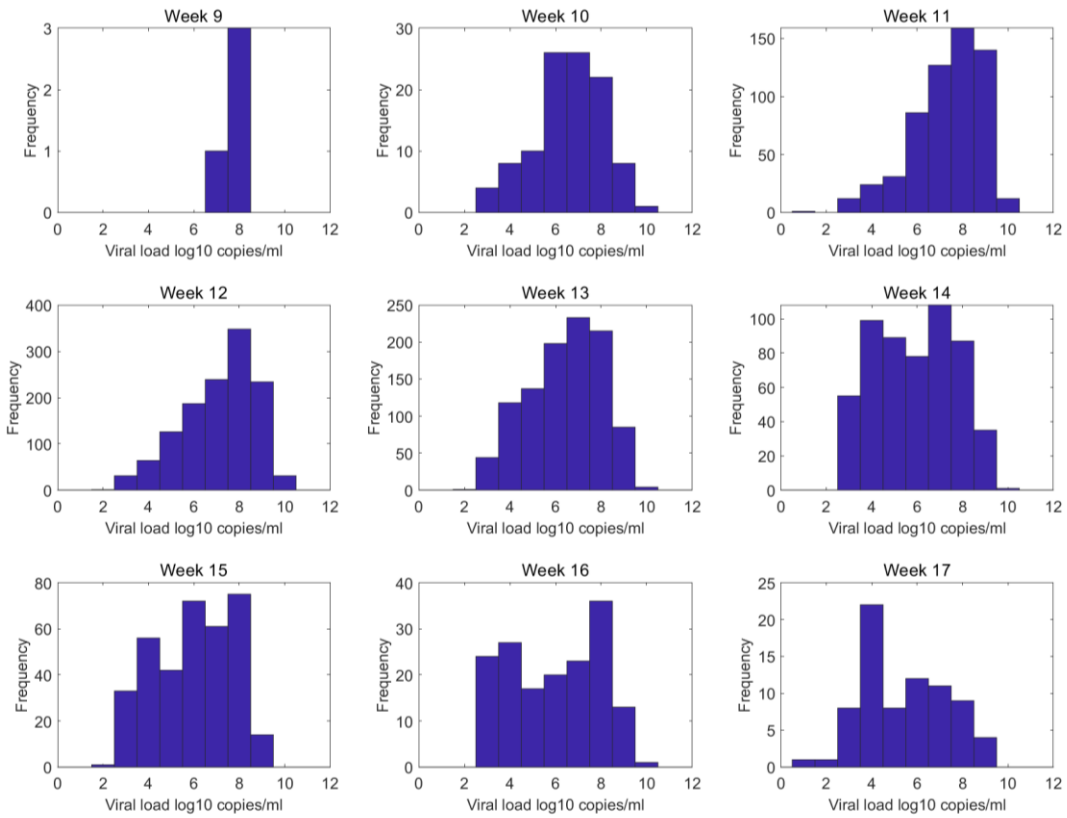

Fig. S5. Frequency distribution of SARS-CoV-2 viral load in Jacot et al. (2020).

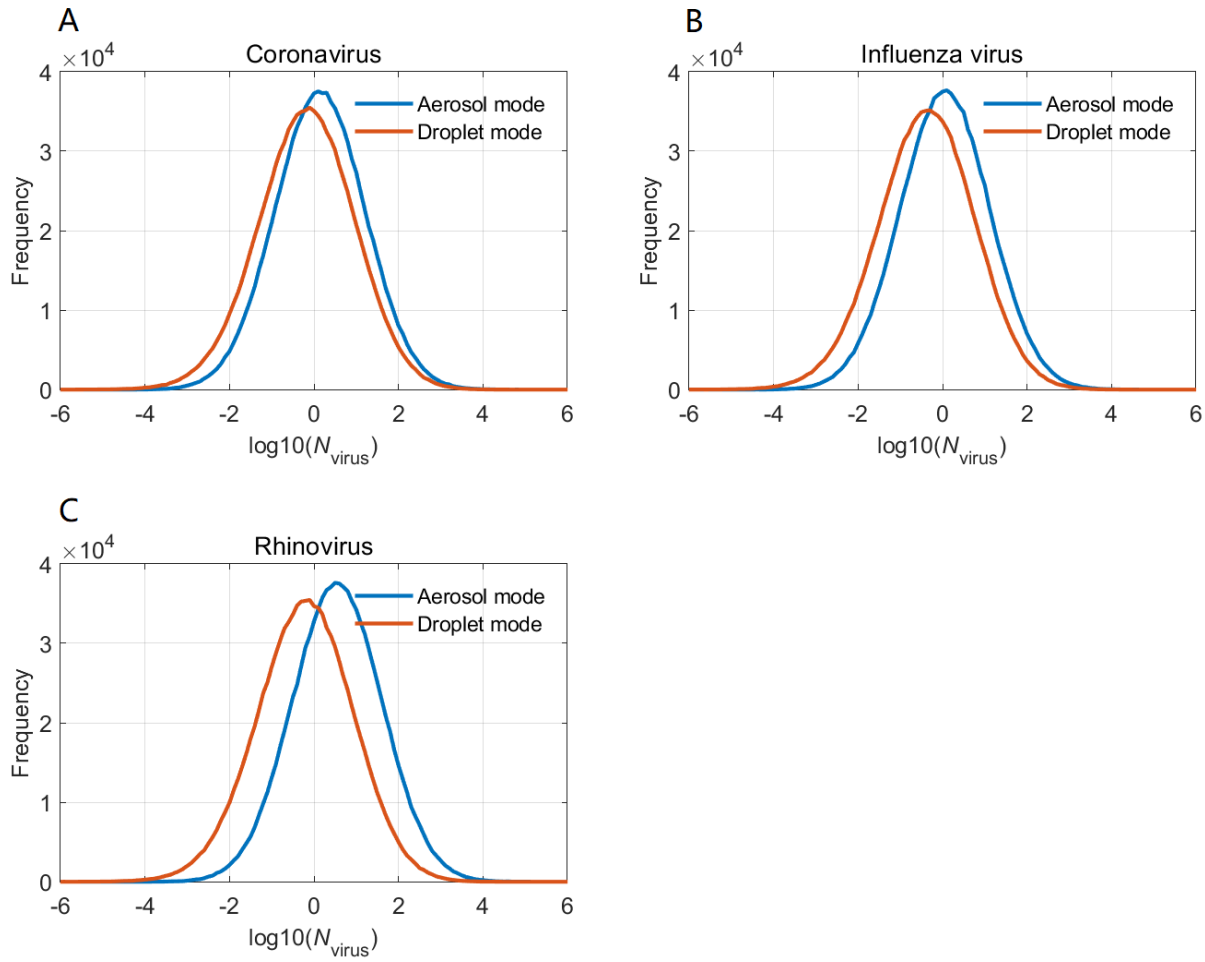

Fig. S6. Frequency distributions of calculated virus number in 30-min exhalation air samples. (**A**), (**B**) and (**C**) show the distribution of coronavirus, influenza virus and rhinovirus, respectively. In each panel, the blue and red lines represent the virus number in aerosol mode and droplet mode, respectively.

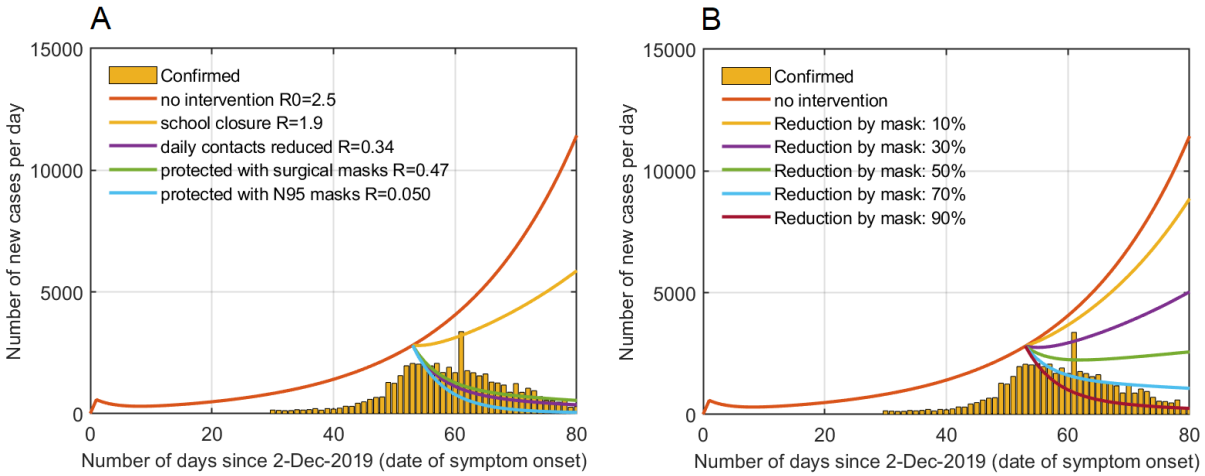

Fig. S7. (**A**) Reported daily new cases in Wuhan and simulated numbers based on different *R* and control measures. (**B**) Simulated daily new cases based on different virus emission reduction rates of masks. In panel (A) and (B), the yellow bars represent the confirmed daily new cases in Wuhan and the colored lines show the simulated daily new cases by the SEIR model with different reproduction number *R*.

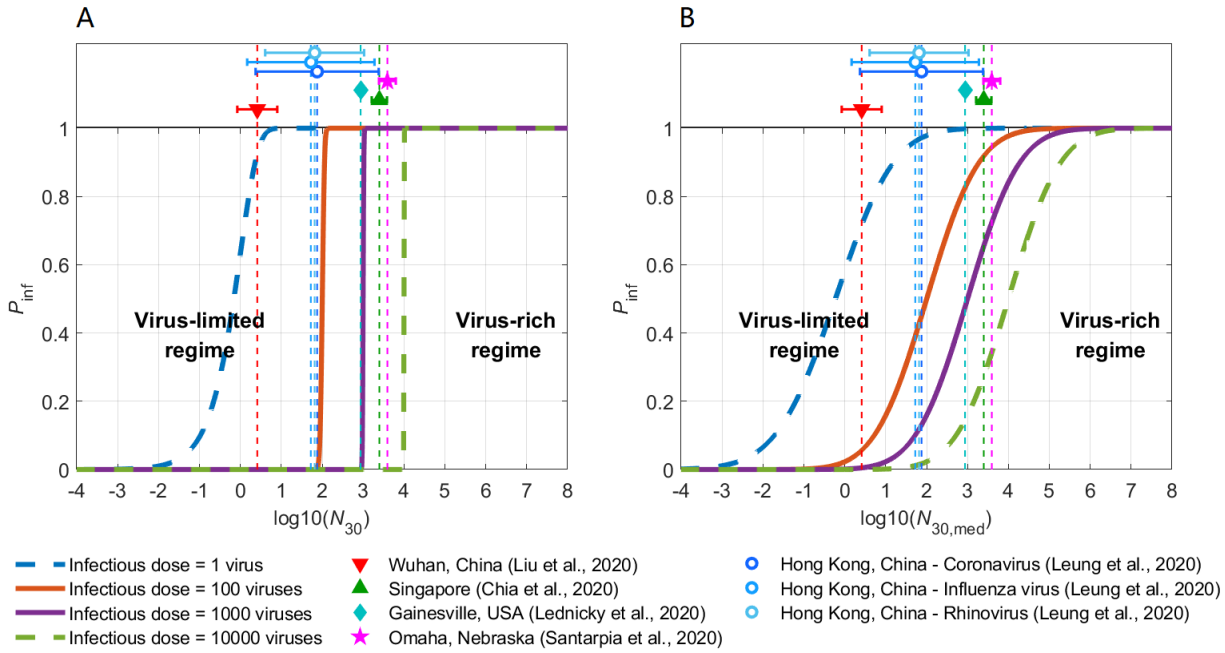

Fig. S8. The same as Fig. 3 except that the infection probability is assumed to be 100% or 0% when N_{30} is above or below the critical dose.

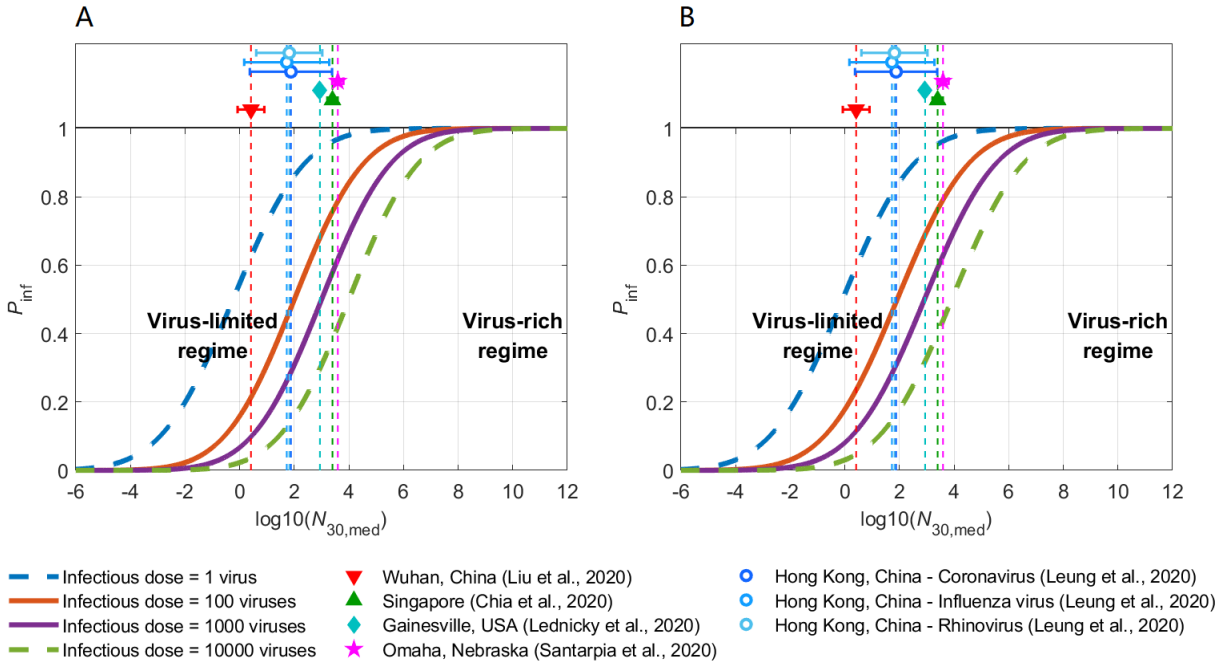

Fig. S9. The same as Fig. 3B and Fig S8B but with a σ of 2.

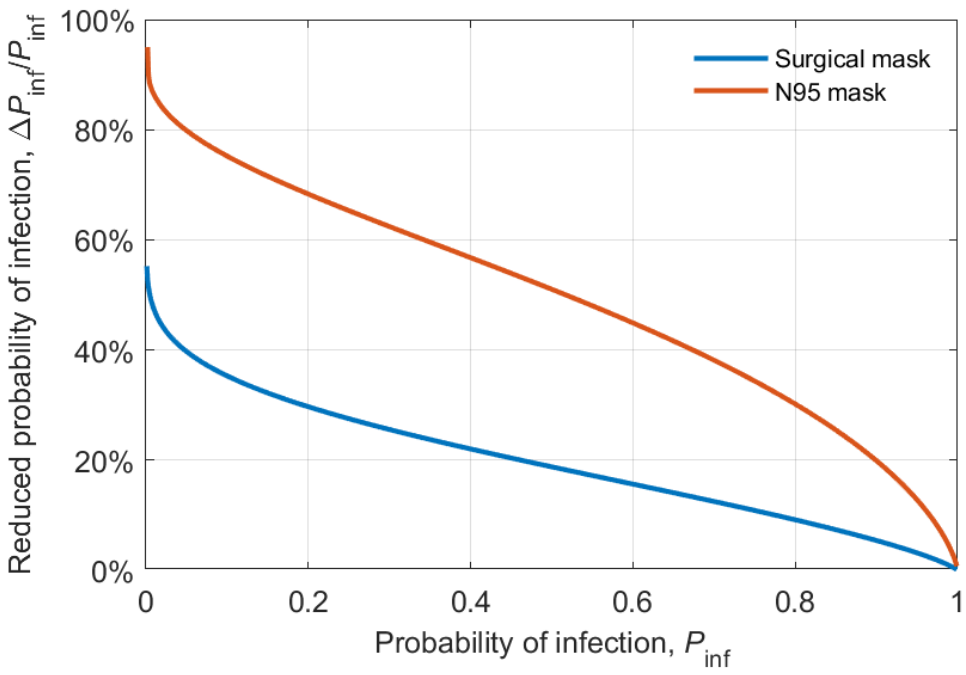

Fig. S10. Reduced chance of COVID-19 transmission with masks. The same as Fig. 4 except for using a σ of ~ 2.

Table S1. Simulated indoor airborne virus concentration in Fangcang Hospital. The indoor airborne concentrations of coronavirus, influenza virus and rhinovirus are simulated for two scenarios: virus emission by patients without wearing masks, and virus emission by patients wearing surgical masks. Median values and 5%, and 95% percentiles are given in the table.

Scenarios	Coronavirus (#/m^3) Median (5%, 95%)	Influenza virus (#/m^3) Median (5%, 95%)	Rhinovirus (#/m^3) Median (5%, 95%)
Virus emission/exhalation by patients without wearing surgical masks	0.658 (3.12e-2, 17.5)	0.466 (2.23e-2, 12.2)	0.995 (4.76e-2, 25.9)
Virus emission/exhalation by patients wearing surgical masks	2.50e-2 (6.70e-4, 1.19)	2.04e-2 (5.32e-4, 0.975)	6.21e-2 (1.50e-3, 3.01)

Table S2. Viral load in exhaled liquids (# mL^{-1}). The viral loads of coronavirus, influenza virus and rhinovirus in aerosol mode (D_w < 5 μm) and droplet mode (D_w > 5 μm) are retrieved based on the measured positive rates of 30-min exhalation samples (1). The individual differences of viral load and particle emission rate are considered in the calculation.

	Coronavirus	Influenza virus	Rhinovirus
D_w < 5 μm *	1.03e6	8.49e5	2.62e6
D_w > 5 μm *	1.55e3	9.69e2	1.42e3

* During the sampling of exhaled particles in Leung et al. (2020) (1), particles with size above and below 5 μm are separated very close to the mouth, thus the cut size (5 μm) of those two groups of particles is considered as wet diameter (D_w).

Table S3. Virus number in the exhalation air samples (#). The virus number in samples is calculated from the retrieved viral loads (Table S2) and total volume of exhaled particles during 30-min sampling.

	Coronavirus	Influenza virus	Rhinovirus
D_w < 5 μm	1.39	1.15	3.55
D_w > 5 μm	0.682	0.429	0.627

Table S4. Emission rate of droplet volume and virus number by infectious individuals. The emission rates of droplets smaller than 5 μm (D_w < 5 μm, D_d < 2.5 μm) and smaller than 20 μm (D_w < 20 μm, D_d <10 um) are given. Three scenarios, patients without wearing masks, patients wearing surgical masks, and patients wearing N95 mask, are assumed in the calculation.

Scenarios	D_w < 5 μm (D_d < 2.5 μm)		D_w < 20 μm (D_d <10 um)	
	$E_{V\text{-}drop}$ (mL h^{-1})	$E_{N\text{-}virus}$ (h^{-1})	$E_{V\text{-}drop}$ (mL h^{-1})	$E_{N\text{-}virus}$ (h^{-1})
No mask	1.11e-6	1.15	3.27E-05	1.20
Surgical mask	2.11e-7	2.18e-1	1.00E-06	2.19e-1
N95 mask	2.29e-8	2.35e-2	9.88E-08	2.37e-2

Table S5. Total infection number and infection rate in Wuhan calculated based on different *R*. The total infection number and infection rate are simulated with the SEIR model. The *R* for the control measures of school closure (*R*=1.9) and daily contacts reduced (*R*=0.34) are reported in Zhang et al. (2020) (6). And the *R* for the control measures of wearing surgical masks (*R*=0.46) and N95 masks (*R*=0.049) are calculated assuming that *R* is proportional to the emission rate of virus-containing droplets.

	R	Total infection number	Total infection rate
No intervention	2.5	9.89E+06	89.3%
School closure	1.9	8.43E+06	76.1%
Daily contacts reduced	0.34	8.69E+04	0.785%
Protected with surgical masks	0.46	1.00E+05	0.903%
Protected with N95 masks	0.049	6.81E+04	0.614%

Table S6. Total infection number and infection rate in Wuhan calculated assuming different virus reduction rates of masks. The total infection number and infection rate are simulated with the SEIR model. The reproduction number *R* is assumed to be proportional to the emission rate of virus-containing droplets.

Reduction rate of mask	*R*	Total infection number	Total infection rate
10%	2.25	9.46E+06	85.4%
30%	1.75	7.91E+06	71.4%
50%	1.25	4.21E+06	38.0%
70%	0.75	1.82E+05	1.65%
90%	0.25	7.94E+04	0.717%

Table S7. Indoor concentration (C_{virus}) and 30-min inhaling number (N_{30}) of SARS-CoV-2 RNA copies in Fangcang Hospital. The table is modified from Liu et al. (2020) (11). Room 1 and 2 are Protective Apparel Removal Room, and Room 3 is Medical Staff's Office. In the calculation of N_{30}, the total volume of inhaled air in 30 min is assumed to be 240 L.

	Mode	Room 1	Room 2	Room 3
C_{virus} (# m^{-3})	Aerosol mode (D_{amb} < 2.5 μm) *	41	13	10
	Droplet mode (D_{amb} > 2.5 μm) *	1	7	10
N_{30} (#)	Aerosol mode (D_{amb} < 2.5 μm) *	9.8	3.1	2.4
	Droplet mode (D_{amb} > 2.5 μm) *	0.24	1.7	2.4

* In this study, the aerosol mode and droplet mode are defined as particles with wet diameter (D_w) smaller than 5 μm and lager than 5 μm, respectively. After being emitted, respiratory particles lose water and dry to ~ half of the initial particle size (12). Therefore, the boundary of these two modes for ambient particles is at ambient diameter (D_{amb}) of ~2.5 μm.

References

1. N. H. L. Leung et al., Respiratory virus shedding in exhaled breath and efficacy of face masks. Nature Medicine 26, 676-680 (2020).
2. M. O. Fernandez et al., Assessing the airborne survival of bacteria in populations of aerosol droplets with a novel technology. Journal of The Royal Society Interface 16, 20180779 (2019).
3. D. Jacot, G. Greub, K. Jaton, O. Opota, Viral load of SARS-CoV-2 across patients and compared to other respiratory viruses. Microbes and Infection https://doi.org/10.1016/j.micinf.2020.08.004 (2020).
4. Y. Drossinos, N. I. Stilianakis, What aerosol physics tells us about airborne pathogen transmission. Aerosol Science and Technology 54, 639-643 (2020).
5. G. Chowell, N. W. Hengartner, C. Castillo-Chavez, P. W. Fenimore, J. M. Hyman, The basic reproductive number of Ebola and the effects of public health measures: the cases of Congo and Uganda. Journal of Theoretical Biology 229, 119-126 (2004).
6. J. Zhang et al., Changes in contact patterns shape the dynamics of the COVID-19 outbreak in China. Science 368, 1481-1486 (2020).
7. H. Wang et al., Phase-adjusted estimation of the number of Coronavirus Disease 2019 cases in Wuhan, China. Cell Discovery 6, 1-8 (2020).
8. S. A. Grinshpun et al., Performance of an N95 filtering facepiece particulate respirator and a surgical mask during human breathing: two pathways for particle penetration. Journal of occupational and environmental hygiene 6, 593-603 (2009).
9. A. Weber et al., Aerosol penetration and leakae characteristics of masks used in the health care industry. American Journal of Infection Control 21, 167-173 (1993).